

8B.5

EXAMING TRENDS IN SATELLITE-DETECTED OVERSHOOTING TOPS AS A POTENTIAL PREDICTOR OF TROPICAL CYCLONE RAPID INTENSIFICATION

Sarah A. Monette* and Christopher S. Velden
Cooperative Institute for Meteorological Satellite Studies, Madison, WI

Kyle S. Griffin
University at Albany, Albany, New York

Christopher M. Rozoff
Cooperative Institute for Meteorological Satellite Studies, Madison, WI

1. INTRODUCTION

One of the essential ingredients to the intensification of tropical cyclones (TCs) is vigorous convection with associated latent heat release through condensation processes (Adler and Rodgers 1977, Kuo 1965). Identifying and quantifying active convection in the tropics has been attempted in a variety of ways, mainly through the use of satellites (Steranka et al. 1986, Alcala and Dessler 2002, Liu and Zipser 2005, Romps and Kuang 2009, Olander and Velden 2009).

This paper examines a new geostationary satellite-based method, employing Infrared window (IRW) imagery and an objective overshooting top (OT) detection algorithm in an effort to quantify vigorous tropical convection associated with TCs; particularly prior to their rapid intensification (RI) stages. The OT detection algorithm is a modification of an existing algorithm originally developed for mid-latitude severe weather applications (Bedka et al. 2010). The OT detection criteria are retuned for use in the tropics in an attempt to identify the frequency and trends in OTs during Atlantic TCs. Correlations between OT trends and subsequent RI are then investigated to assess the utility of an OT-based scheme as a possible tool for probabilistic forecasting of RI events.

2. DATA

A geostationary satellite-derived OT detection algorithm is utilized to identify OT activity associated with Atlantic tropical disturbances. The OT detection algorithm utilizes the 11- μ m infrared window (IRW) brightness temperature (BT) observed at a 4-km spatial resolution for the

Geostationary Observing Environmental Satellite (GOES) satellite and a 3-km spatial resolution METEOrological SATEllite (METEOSAT). First, the algorithm identifies candidate OTs, which are IRW pixel minima at least 215 K or colder. Next, the surrounding anvil is sampled at an 8 km radius in 16 radial directions. Candidate anvil pixels must have a BT of at least 225 K, and at least 9-out-of-16 potential anvil pixels must satisfy this criterion. These pixels are used to calculate the mean anvil BT, and the candidate OT classified as an OT if the minimum pixel BT and anvil-mean BT difference is at least 9 K.

To cover the Atlantic hurricane development region, multiple geostationary satellite scans are employed. The GOES-E Contiguous United States (CONUS) scan, with a 15-min temporal resolution, is utilized with a scan range from 110° W to 62° W down to 15° N. Beginning in 2004, METEOSAT imagery also became available at 15-min temporal resolution and is used east of 55° W (the large viewing angle west of this range begins to affect OT sampling). TCs located between 55° W and 62° W are analyzed with the GOES-E Northern Hemisphere (NH) scan, which is limited to 30-min temporal resolution. For cases prior to 2004, TCs east of 62° W are analyzed by the GOES-E NH scan up to an easternmost extent of 40° W. Finally, TCs located west of 62° W but south of 15° N are also analyzed by the GOES-E NH scan.

This study includes a dependent analysis of 100 Atlantic TCs within the GOES CONUS viewing domain from 1995-2005 and 2008 reaching at least tropical storm (TS) strength plus 9 TCs from 2004-2005 and 2008 whose entire track falls within the METEOSAT scan. A smaller subset consisting of 23 Atlantic TCs from 2006 and 2007 is used in an independent test of performance, chosen to benchmark against the results of the operational Rapid Intensification Index (RII) model presented by Kaplan et al. (2010). For validation, interpolated National Hurricane Center (NHC) Best Track intensities

*Corresponding author address: Sarah Monette, Cooperative Institute for Meteorological Satellite Studies, 1225 W. Dayton St., Madison, WI 53706
E-mail: sarah.monette@ssec.wisc.edu

(maximum 1-min sustained 10-m winds, MSW) are used. RI is defined based on three MSW thresholds: +25 knots, +30 knots, and +35 knots in 24 hours.

Similar to procedures used in Kaplan et al. (2010) and Rozoff and Kossin (2011), OTs are not analyzed when the TC center is within $t=12$ to $t=24$ hours of land. OTs are also not analyzed when the TC is of Category 4 or 5 intensity, the TC is either subtropical or extratropical, or the system is categorized as an open wave (based on NHC Best Track data).

3. PREDICTING RAPID INTENSIFICATION TO BEGIN IN THE SUBSEQUENT 24 HOURS

The first approach examined in this study is to forecast the probability of an RI event beginning sometime in the subsequent 24 hours from analysis time. For verification purposes, we define an RI event as a time period of 24 h or longer during which a TC intensifies at a rate at least 25 kt 24 h^{-1} . If this rate is maintained for longer than 24 h, then the RI event can last as long as the intensity has increased by a minimum rate of 25 kt in the 24 h immediate preceding the ending time. Subsequently, an RI event can be viewed as a series of overlapping 24-h periods with intensity changes greater than the examined RI threshold, independent of intensity changes over shorter periods within or beyond the ends of the period.

Optimal forecast parameters for this approach of predicting RI are found by comparing different parameter combinations. Each combination includes one of the following:

- OT BT minimum and OT-anvil temperature difference (BTD) minimum: 215 K and 9 BT, 205 K and 9 BT, 200 K and 9 BT, 215 K and 12 BT, 215 K and 15 BT
- Radii from disturbance center: 100 km, 150 km, 200 km, 300 km, 500 km
- OT averaging timeframes: 3 h, 6 h, 12 h, 24 h,
- Selected OT scan^{-1} thresholds

These different combinations are compared using their Peirce Skill Score (PSS), with a PSS of 1 (0) representing a perfect (random) RI forecast (Wilks 2006). The PSS is equal to the probability of detection (POD), the ratio of the correctly forecasted RI occurrences to the actual number of RI occurrences, minus the probability of false detection (POFD), which is the number of false alarms divided by the total number of non-occurrences. The False Alarm Ratio (FAR) is calculated by dividing the number of incorrect forecasts of RI by the total number of RI forecasts.

Both the POFD and FAR have negative orientations, thus lower values are preferred.

In this analysis, an RI forecast is made at the beginning of each hour. Analysis of the 15-min interpolated data found that 52% (25-kt), 62% (30-kt), and 75% (35-kt) of RI events extend beyond the synoptic hours. Thus, this “hourly forecast” could provide a more precise analysis of when RI will start or end. Introduced for this forecast method are additional methods of evaluation. A modified POD, called Running Probability of Detection (RPOD), is calculated, as the “hourly” forecast has the potential to indicate or miss RI 24 times before it occurs. Thus, the RPOD is the total number of times RI is correctly forecasted to occur, divided by the total number of opportunities to correctly forecast RI. For example, if in the 24 hours prior to an RI event, an hourly forecast OT scan^{-1} threshold is exceeded 6 times, the RPOD is $6/24$ or 25%. The Running Peirce Skill Score (RPSS) is calculated by subtracting the POFD from the RPOD.

Based on the 1995-2005 & 2008 developmental sample results, the optimal thresholds for predicting the onset of 25-knot RI are: 3-hour average of 2.5 OTs scan^{-1} , with an OT BT colder than or equal to 215 K and a BT of 9 K within a 200 km radial disk of the TC center. With a POD of 50.0% and FAR of 72.4%, the forecast is skillful, as indicated by positive PSS (0.420) and RPSS (0.162) values. The RPSS values are much below the PSS values due to the low RPOD, as seen in Figure 1.

The optimal thresholds for predicting 30-kt RI are: a 6-hour average of 2.5 OTs scan^{-1} with a BT of 215 K or colder and a BT greater than or equal to 9 K within 200 km of the TC center. From Figure 1, this RI threshold has a POD of 50.0%, indicating this forecast has a similar detection rate to the 25-kt forecast with a comparable FAR of 74.0%. Again, this forecast is still skillful, based on the positive PSS (0.418) and RPSS (0.119) values.

Results from the 35-kt RI onset forecasts are also shown in Figure 1. Optimal thresholds for predicting RI of this magnitude are: 3-hour average of 2 OTs scan^{-1} with a BT of 205 K or colder and a BT greater than or equal to 9 K within 200 km of the TC center. Of the very limited sample of 4 events available for analysis, the OTs RI correctly forecasted 2, for a POD of 50.0%. This forecast is skillful, based on a positive PSS value of 0.367, however the RPSS value is negative (-0.090), a result of the lower RPOD. Thus, while having accuracy at predicting which TCs will undergo major RI, the OT-based index

lacks consistency in continually predicting RI in the 24 hours preceding the onset of RI.

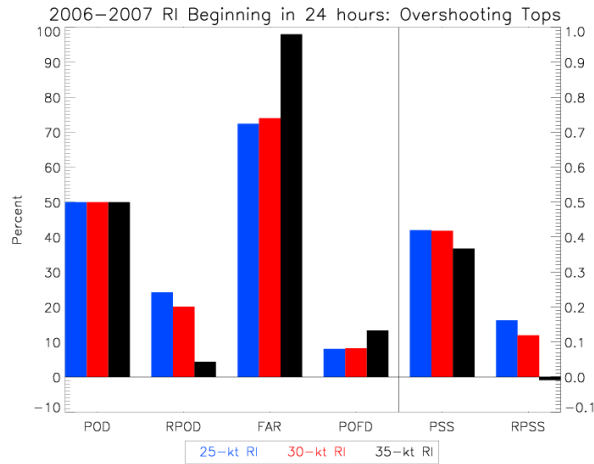


FIG 1. Probability of Detection (POD), Running Probability of Detection (RPOD), False Alarm Ratio (FAR), Probability of False Detection (POFD), Peirce Skill Score (PSS), and Running Peirce Skill Score (RPSS) for the OT RI forecasted to begin in the subsequent 24 hours.

4. PREDICTING RAPID INTENSIFICATION TO OCCUR IN THE SUBSEQUENT 24 HOURS

Another method of forecasting RI mimics the operational Rapid Intensification Index (RII), in that an intensification rate of at least 25-kt is forecast to begin and complete within the 24 hours immediately following the forecast. These forecasts are made on the synoptic hours and found by comparing the PSS of the combinations presented in the previous section.

The OT algorithm is tested as a predictor of 24-h RI completion on an independent sample of TCs from 2006-2007. Based on this dataset, the optimal settings for 25-kt, 30-kt, and 35-kt RI are: 6-hour average of 2.5 OTs scan⁻¹ with a BT of 215 K or colder and a BTD greater than or equal to 9 K within 300 km of the TC center. The resulting skill for these OT RI forecasts, compared to the RII, can be seen in Figure 2. The POD for the RI forecasts based solely on OTs, ranges from 23.1% to 37.5%, compared to 15%-59% for the RII. While the OTs have a higher POD for 35-kt RI than the RII, the FAR is also much higher at 98.0% compared to 71% for the RII. The OT RI forecast FAR ranges from 84.1% to 96.0% with a POFD of 20.9% to 27.7%. Overall, the PSS for the OT based forecast is below the PSS for the RII, indicating a less accurate forecast. This is an expected result due to other important environmental factors being accounted for by the RII scheme.

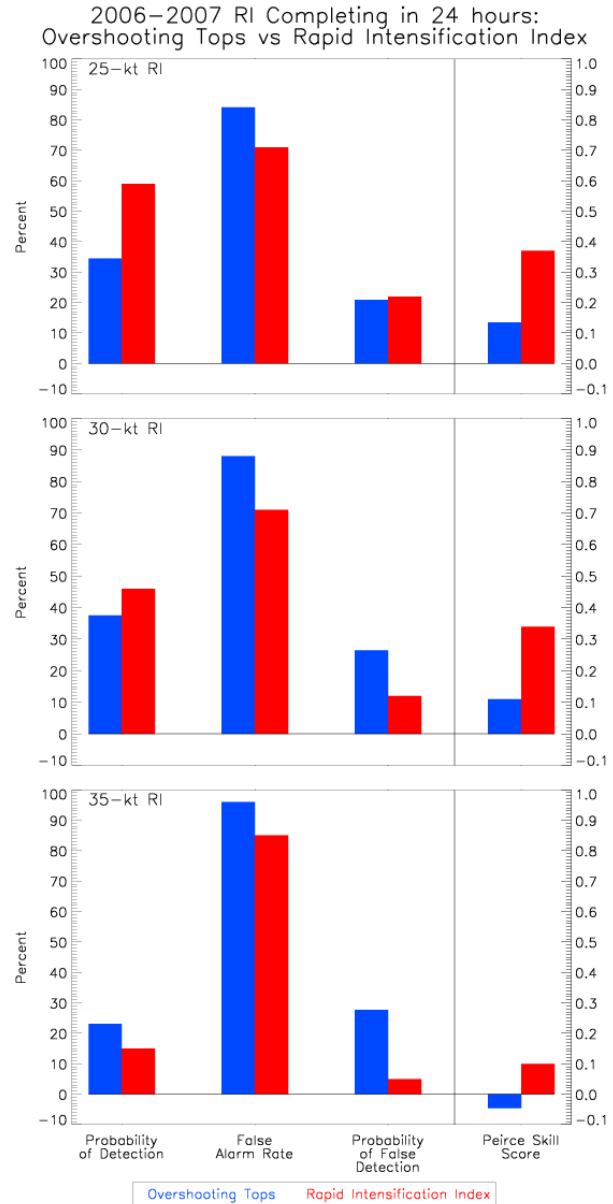


FIG 2: Probability of Detection, False Alarm Ratio, Probability of False Detection, and Peirce Skill Score for the OT RI forecasts (blue) compared to the Rapid Intensification Index (red). RI is forecasted to begin and complete in the subsequent 24 hours.

5. ADDITION TO A LOGISTIC REGRESSION PREDICTION SCHEME

To investigate the OTs impact on a multiple parameter prediction scheme like the RII, using the same 1995-2005 & 2008 dataset and case sample, OT data is provided to the logistic regression algorithm from Rozoff and Kossin (2011). Three-hour average OTs within 50 km radius and 6-h average OTs within 200 km of the TC center prior to synoptic time are added to the 7 predictors defined by Table 1 in Rozoff and Kossin

(2011) for forecast skill verification. The impact of the OTs is analyzed using the Brier Skill Score (BSS). The BSS compares the difference between predicted probabilities, with the

$$\text{BSS} = 1 - \frac{\text{BS}_{\text{log. reg.}}}{\text{BS}_{\text{ref}}} \quad \text{where } \text{BS} = \frac{1}{n} \sum_{k=1}^n (y_k - o_k)^2$$

and y_k and o_k are the predicted and observed probabilities (Wilks 2006). For this research, the BS_{ref} represents the Brier Score of the climatological formation probability. Upon adding the OTs, the resulting BSS for the 25-kt and 35-kt RI forecasts increase by 3.2% and 1.6%, respectively, while the BSS for 30-kt RI does not significantly change (0.3% increase).

A reliability diagram can better indicate in which situations the OTs have a positive contribution to the logistic regression forecast scheme which is not highlighted by the scalar BSS. Seen in Figure 3, each reliability diagram, shown in the left panels, the 45° dotted-dashed line represents perfect reliability for all forecast probabilities. Perfect reliability is defined as the verifying percent equaling the forecasted probability. For example, perfect reliability for events with a 10% forecasted probability has 10% verifying. Points above the dotted-dashed line indicating forecast probabilities that are too low compared to observed probabilities (for example, 50% forecasted probability with 80% verifying) and points below the dotted-dashed line indicating forecast probabilities that are too high (80% forecasted probability with 50% verifying, for example). For 25-kt and 30-kt RI forecasts, the addition of the OTs produces a more reliable forecast at higher probabilities ($\geq 50\%$), with the exception of probabilities between 70% and 80%. The results for 35-kt RI are mixed, even though the included OT parameters are chosen based on this RI threshold.

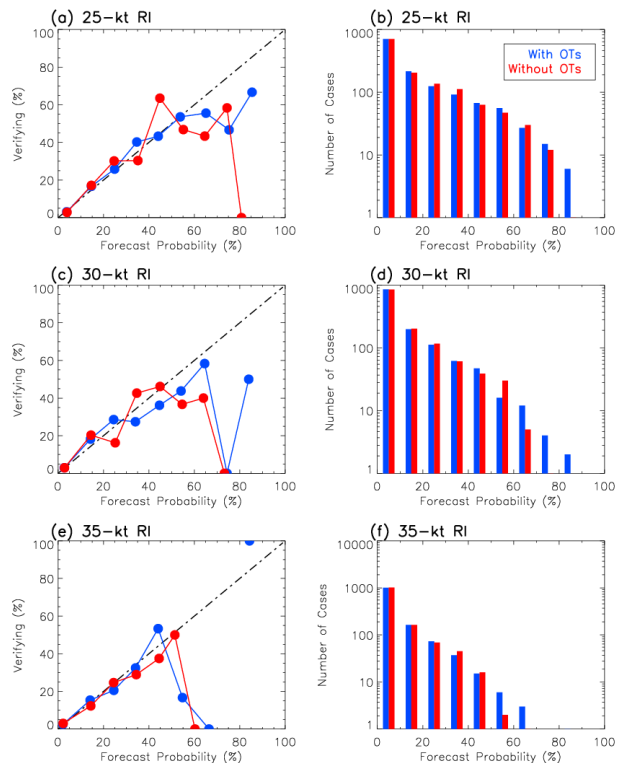


FIG 3. Reliability diagrams from the logistic regression models with OTs (black) and without OTs (dark gray) for RI thresholds of (a) 25, (c) 30, and (e) 35 kts 24 h^{-1} and the corresponding number of forecasts for (b) 25, (d) 30, and (f) 35 kts in 24 h^{-1} for forecast probabilities between 0%-10%, 10%-20%, ..., 90%-100%.

Acknowledgements

This research is funded by the NOAA GOES-R Proving Ground Program Contract No. NA06NES4400002: Fund 144PH46 and NSF grant AGS-0935830. The authors would like to thank Kristopher Bedka (Science Systems and Applications, Inc.) for suggestions related to adapting his original OT detection algorithm to the tropics.

References

- Adler, R. F. and E. B. Rodgers, 1997: Satellite-Observed Latent Heat Release in a Tropical Cyclone. *Mon. Wea. Rev.*, **105**, 956-963.
- Alcala, C. M., and A. E. Dessler, 2002: Observations of deep convection in the tropics using the Tropical Rainfall Measuring Mission (TRMM) precipitation radar. *J. Geophys. Res.*, **107**, doi:10.1029/2002JD002457.
- Bedka, K. M., J. Brunner, R. Dworak, W. Feltz, J. Otkin and T. Greenwald, 2010: Objective Satellite-Based Overshooting Top Detection Using Infrared Window Channel Brightness Temperature Gradients. *J. Appl. Meteor. And Climatol.*, **49**, 181-202.

Kaplan, J., M. DeMaria and J. A. Knaff, 2010: A Revised Tropical Cyclone Rapid Intensification Index for the Atlantic and Eastern North Pacific Basins. *Wea. Forecasting*, **25**, 220–241.

Kuo, H. L., 1965: On Formation and Intensification of Tropical Cyclones through Latent Heat Release by Cumulus Convection. *J. Atmos. Sci.*, **22**, 40-63.

Liu, C., and E. J. Zipser, 2005: Global distribution of convection penetrating the tropical tropopause. *J. Geophys. Res.*, **110**, D23104, doi:10.1029/2005JD006063.

Olander, T. L. and C. S. Velden, 2009: Tropical Cyclone Convection and Intensity Analysis Using Differenced Infrared and Water Vapor Imagery. *Wea. Forecasting*, **24**, 1558–1572.

Romps, D. M., and Z. Kuang, 2009: Overshooting convection in tropical cyclones, *Geophys Res. Lett.*, **36**, L0984, doi:10.1029/2009GL037396.

Rozoff, C. M., and J. P. Kossin, 2011: New probabilistic forecast models for the prediction of tropical cyclone rapid intensification. *Wea. Forecasting*, **26**, 677–689.

Steranka, J., E. B. Rodgers, and R. C. Gentry, 1986: The Relationship between Satellite Measured Convective Bursts and Tropical Cyclone Intensification *Mon. Wea. Rev.*, **114**, 1539-1546.

Wilks, D. S., 2006: Statistical Methods in the Atmospheric Sciences. 2nd ed. Academic Press, 627 pp.